Polymer Vol. 39 No. 24 pp. 6099–6108, 1998
0032-3861/98/$ – see front matter

PII: S0032-3861(98)00039-1

Interfacial characterization of compatibilized PVC/SBR blends by solid-state n.m.r. and TEM

Shui-Han Zhu[a], Man Ken Cheung[†b] and Chi-Ming Chan[a,*]
[a]*Department of Chemical Engineering, Advanced Engineering Materials Facility, The Hong Kong University of Science and Technology, Clear Water Bay, Hong Kong*
[b]*Department of Applied Biology and Chemical Technology, The Hong Kong Polytechnic University, Hung Hom, Kowloon, Hong Kong*
(Received 24 July 1997; revised 3 December 1997; accepted 15 December 1997)

At ambient temperature, n.m.r. relaxation measurements of poly(vinyl chloride) (PVC)/styrene-butadiene rubber (SBR) blends, compatibilized by acrylonitrile-butadiene rubber (NBR), reveal two rotating-frame spin-lattice relaxation ($T_{1\rho}^{H}$) components for the methylene protons of rubbers (SBR + NBR). The short $T_{1\rho}^{H}$ component may be interpreted as the contribution of the rubbers in the PVC/rubbers interface. The long $T_{1\rho}^{H}$ component is attributed to the rubbers isolated from PVC. As sulfur concentration increases, the long $T_{1\rho}^{H}$ decreases due to increasing restraints imposed on the rubber chains by crosslinking, but the fraction of rubbers with short $T_{1\rho}^{H}$ increases, indicating that the rubber fraction at the interface increases.

The TEM micrographs of stained and unstained samples show identical morphological information. For the unstained samples, the PVC and SBR regions appear as dark and light areas, respectively. The dehydrochlorination of PVC in the blends under an electron beam reduces the contrast between the dark and light areas, producing an inversion of contrast. However, when the blends are compatibilized by NBR, the deterioration rate of the contrast slows down significantly. As the dark PVC regions become lighter, dark boundaries are visible between the PVC and SBR phases. In particular, the dark boundaries remain visible upon extended exposures of electron beam irradiation. This is explained by the stabilizing effect of the higher rubber concentration in the interfacial regions between PVC and SBR. The TEM micrographs of the unstained samples for this system provide a unique method to show the segregation of rubbers at the interfacial regions between PVC and SBR for the compatibilized blends.

(Keywords: thermoplastic elastomer; dynamic vulcanization; polymer blends)

INTRODUCTION

Solid-state nuclear magnetic resonance (n.m.r.) spectroscopy allows easy sample preparations and direct measurements of magnetization signals in solid samples without the complication of solvent as in solution-state n.m.r.. Sophisticated instrumentation techniques, such as magic angle spinning (MAS), high power dipolar-decoupling (DD), cross polarization (CP) and multiple-pulse sequences, that can eliminate specific Hamiltonian interactions selectively, make n.m.r. a powerful tool for the analysis of complex polymer blends[1–6]. The magnetization transfer and relaxation of nuclear spins in solid polymer blends are widely utilized as sensitive probes to investigate the spatial heterogeneities and the local constituent compositions[7–15].

The proton spin-lattice relaxation time in the laboratory frame (T_1^H) is sensitive to molecular motions at hundreds of megahertz near the Larmor frequency[1,2]. The proton spin-lattice relaxation time in the rotating frame ($T_{1\rho}^H$) and the spin–spin relaxation time (T_2^H) are sensitive to chain motions at tens of kilohertz. T_2^H has been shown to be well correlated to crosslinking density in rubber, in other words it is sensitive to constraints on long-range cooperative chain motions[16,17]. However, interpretation of proton relaxation times in terms of chain motions for solid polymers below their glass transition temperatures is very complicated because proton–proton dipolar interactions can broaden the linewidth by tens of kilohertz. Proton spin diffusion also makes correlation of proton relaxation times to chain motions in solid polymers difficult. The ^{13}C relaxation times are better correlated to chain motions than proton relaxation times[18–21]. Nevertheless, ^{13}C n.m.r. studies of chain motions in solid polymer blends are rare[22].

The effect of proton spin diffusion on proton T_1^H and $T_{1\rho}^H$ in solid polymer blends, however, gives valuable information about the scale of miscibility between two polymer components[11–15,23–25]. When the domain size is larger than 500–1000 Å, spin diffusion will not be rapid enough to equalize the T_1^H and $T_{1\rho}^H$ from the two components, and so multi-relaxation times will be observed. When the domain size is larger than 50–500 Å, spin diffusion is rapid enough to equalize the T_1^H on the time-scale of T_1^H (typically 100 ms up to 10 s) but not rapid enough to equalize $T_{1\rho}^H$ on the time-scale of $T_{1\rho}^H$ (typically 1–100 ms). Experimentally, a single effective T_1^H will be observed but more than one $T_{1\rho}^H$ will be observed. When the domain size is between 10 and 50 Å or smaller, spin diffusion is rapid enough to equalize both T_1^H and $T_{1\rho}^H$ from the two components, and so single effective relaxation times T_1^H and $T_{1\rho}^H$ will be observed.

Wide-line proton n.m.r. have been used to measure T_1^H and T_2^H in vulcanized PVC/NBR binary blends[26]. Single exponential T_1^H decay was observed because spin diffusion averaged out the spin-lattice relaxation at different regions

* To whom correspondence should be addressed
† To whom NMR questions should be addressed.

to have one observable T_1^H. Fitting the free induction decay (FID) signal by the sum of one Gaussian and two exponential functions, three T_2^H components were measured. The shortest T_2^H derived from the Gaussian function was ascribed to the rigid PVC regions. The mid and longest T_2^H were ascribed to rubber regions of different chain mobility. The mid T_2^H component was attributed to crosslinked regions.

T_1^H and $T_{1\rho}^H$ measurements of unvulcanized PVC/NBR blends with pulse sequences the same as those used in the present study also found single observable T_1^H caused by spin diffusion averaging[27]. However, two-component $T_{1\rho}^H$ relaxations in both PVC and NBR domains were observed. When the subdomains within the PVC or the NBR domain were large so that spin diffusion rate was small relative to the difference in the $T_{1\rho}^H$ relaxation rates, each subdomain would relax independently[28]. The short $T_{1\rho}^H$ component of PVC was assigned to the microcrystalline subdomains. The short $T_{1\rho}^H$ component of NBR was assigned to the subdomains of NBR isolated from the PVC domains. The long-component $T_{1\rho}^H$ values of both PVC and NBR were identical within experimental error, indicative of a region where NBR chains were penetrated into the PVC domains, and where spin diffusion effectively equalized the $T_{1\rho}^H$ values. This present work differs from the above works because both unvulcanized and vulcanized ternary blends of PVC/NBR/SBR are also studied besides PVC/NBR binary blends. Solid-state n.m.r. studies of ternary blends are rare in the literature.

Transmission electron microscopy (TEM) is a powerful tool to study the morphology of multiphase polymers with the staining technique. However, most polymers will undergo chain scission or crosslinking under electron beam irradiation[29–36]. PVC is not stable under an electron beam and the major degradation mechanism is dehydrochlorination[29,30]. Attempts to observe directly the morphology of the PVC blends are few due to the drifting images, which are caused by dehydrochlorination. The decomposition mechanism under electron beam irradiation is different from that due to thermal degradation. A stabilizer, which helps to minimize thermal degradation, has little effect on the dehydrochlorination caused by electron beam irradiation. However, the environment of the PVC and the availability of hydrogen will affect the dehydrochlorination rate or mechanism significantly. It is known that the radiation stability can be improved via blending[32]. The effect is particularly noticeable if the polymers are miscible. For example, a marked decrease in the rate of scission of poly(methyl methacrylate) (PMMA) was observed in the blend of PMMA and styrene-acrylonitrile copolymers[33]. Based on the fact that the dehydrochlorination rate of PVC can be reduced by the presence of NBR or SBR or both[34], we have recently developed a novel method to detect the enhanced rubber concentration at the interface between the PVC and SBR phases. In the present study, the interfacial properties and morphology of PVC/NBR, PVC/SBR and PVC/NBR/SBR blends were characterized by solid-state n.m.r. and TEM.

EXPERIMENTAL

Blends containing poly(vinyl chloride) (PVC) and styrene-butadiene rubber (SBR) with and without acrylonitrile-butadiene rubber (NBR) as the compatibilizer were prepared. The blend containing 50 wt% of PVC, 40 wt% of SBR and 10 wt% of NBR is designated as PVC/NBR/SBR (50/10/40). The curing system contains sulfur as a primary crosslinking agent, 2-mercaptobenzothiazole (MBT) as an accelerator and zinc oxide as an activator. Barium and zinc stearates are the thermal stabilizers for PVC. PVC (K value 67), SBR (Nipol 1502, Zeon Chemicals, Inc. USA), and NBR (Nipol 1053 and 1041 containing 29.5 and 40 wt% acrylonitrile, respectively, Zeon Chemicals, Inc., USA) were used. The mixtures were melt-blended in a Haake mixer 600 at a control temperature of 150°C. Either NBR-29 (acrylonitrile content of 29.5 wt%) or NBR-40 (acrylonitrile content of 40 wt%) was used each time. The Banbury rotors were operated at 30 rpm. A built-in thermocouple inside the mixer chamber showed a higher measured melt temperature of 159–162°C due to viscous heating.

Proton spin-lattice relaxation times in the laboratory (T_1^H) and rotating ($T_{1\rho}^H$) frame were measured by a method of $^1H-^{13}C$ cross polarization at ambient temperature using a 9-T JEOL EX-400 n.m.r. spectrometer. This method permits the determination of the proton relaxation at different carbon sites. In all the experiments, samples were spun at 4–5 kHz in a 6 mm rotor. There were no spinning sidebands. The ^{13}C spectrum was acquired after a $^1H-^{13}C$ cross polarization contact for 1.0 ms. The predelay times for T_1^H and $T_{1\rho}^H$ measurements were 9 and 7 s, respectively. The 90° pulsewidth for ^1H was 5.0 μs. Adamantane was used as an external reference; it has two peaks at the dispersal spectrum: 29.5 and 38.6 ppm relative to tetramethylsilane. Sixty four scans and one dummy scan were used.

The TEM samples were prepared by a ultracryomicrotome (Ultracut R, Leica) at −120°C. The nominal advance after trimming was set at 80 nm. The sections at the knife edge were moved to the base clearings of the knife using a hair-probe and collected on copper grids by a loop of sucrose solution. The sections on copper grids were stained by OsO_4 vapour for 40 min, and coated with a 40 nm layer of carbon.

RESULTS AND DISCUSSION

n.m.r. relaxation measurements

Four resonant peaks were obtained in the ^{13}C CP-MAS spectra of PVC/NBR, PVC/SBR and PVC/NBR/SBR blends: 130, 57, 46 and 33 ppm relative to TMS. They are broad overlapping peaks from the various conformational and configurational environments of the blend components. *Figure 1* shows two ^{13}C spectra for the PVC/NBR-29/SBR (50/10/40) and PVC/NBR-40/SBR (50/10/40) blends vulcanized by S/MBT/ZnO = 2.0/0.5/4.0 phr. The two spectra are quite similar in spite of the different compatibilizers used. The peaks at 130 and 33 ppm are assigned to the CH=(methine) and CH_2 (methylene) groups in the rubber, respectively. The contribution of methine signals in the rubber comes from the phenyl ring carbon in the styrene residue, the double bonds in the butadiene and the C≡N substituted carbon. Signals from SBR and NBR are overlapped and cannot be resolved by the present methods. The peaks at 57 and 46 ppm are assigned to the CHCl (chloromethylene) and CH_2 groups in the PVC. All the peak assignments are similar to those in the literature[38–40], considering the different experimental conditions. The proton relaxations at different carbon sites can be resolved to yield detailed information on the blend components.

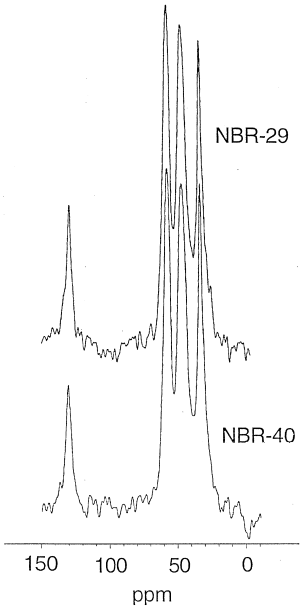

Figure 1 ^{13}C NMR spectra of the PVC/NBR/SBR (50/10/40) blends vulcanized by S/MBT/ZnO = 2.0/0.5/4.0 phr. (a) NBR-29 and (b) NBR-40

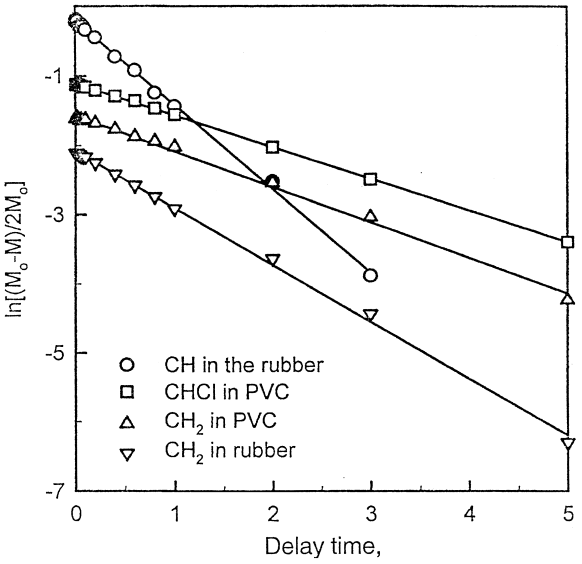

Figure 3 Semilog plots of the protonated carbon magnetization after CP as a function of delay time in T_1^H measurement for the unvulcanized ternary PVC/NBR-29/SBR (50/10/40) blends (for clarity, the lower three lines have been shifted downward 1.0, 1.5 and 2.0, respectively)

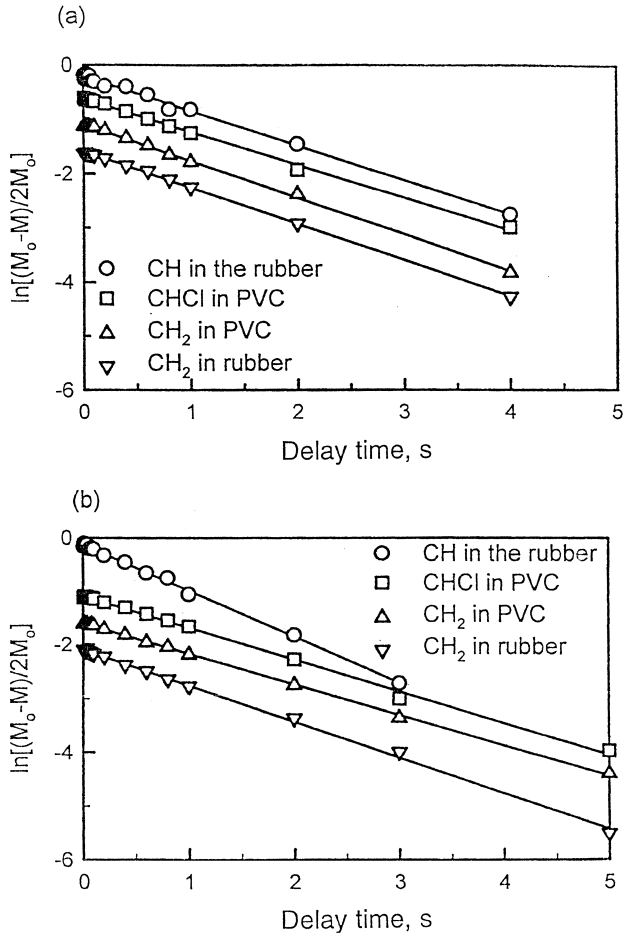

Figure 2 Semilog plots of the protonated carbon magnetization after CP as a function of delay time in T_1^H measurement for the unvulcanized binary PVC/NBR (50/50) blends: (a) NBR-40 (for clarity, the lower three lines have been shifted downward by 1.0, 1.5 and 2.0, respectively); (b) NBR-29 (for clarity, the lower three lines have been shifted downward by 0.5, 1.0 and 1.5, respectively)

T_1^H *measurement*

In a conventional ^1H n.m.r. spectrum, only the average relaxation time will be obtained. For the present CPMAS ^{13}C spectra, the protons are resolved according to the atomic environment. The ^{13}C magnetization decay after CP as a function of delay time is a reflection of the attached proton magnetic relaxation[21–23]. As exponential decay is usually expected, the relaxation time was determined from the slope of a semilog plot of the magnetization decay as a function of delay time. *Table 1* lists the T_1^H of the pure components in specific carbon groups before mixing.

The semilog plots of the magnetization decay as a function of delay time for the various protons attached to different sites in the PVC/NBR (50/50) blends are shown in *Figure 2a–b*. For the PVC/NBR-40 (50/50) blend (*Figure 2a*), all the protons, either in the PVC or in the NBR-40 relax at the same rate, as one can tell from the parallel lines in the plots. The spin diffusion in the blend is so effective as to completely average out the relaxation rate differences at different protonated carbon sites. The T_1^H results indicate that the PVC/NBR-40 is homogeneous throughout and that the different protonated sites of the NBR-40 and the PVC are indistinguishable — the phase boundaries of NBR-40 and PVC disappear in the T_1^H scale. The values for T_1^H of CHCl and CH_2 groups of PVC in the blends are smaller than those of the pure PVC because of the averaging by the efficient proton spin diffusion. Due to the same reason, the values for T_1^H of the rubber increases due to the presence of the rigid PVC. In the case of the unvulcanized PVC/NBR-29 (50/50) blends, slightly different slopes were found in the semilog plot (*Figure 2b*) for the protons of the PVC and the NBR-29. The size of the microheterogeneity in the blend cannot be completely spanned by the proton spin diffusion in the T_1^H timescale. Thus the protons of the PVC and the NBR-29 relax at different rates, as shown in *Table 1*. In the case of the PVC/SBR (50/50) blends, the T_1^H for the CHCl and CH_2 of the PVC and the CH group of SBR are very similar to those measured for the pure components. However, T_1^H of the CH_2 group in SBR is significantly longer than that of the pure component.

Table 1 Effect of NBR-29 on the T_1^H (s) of the blends unvulcanized and vulcanized by S/MBT/ZnO/ = 0.5/0.5/1.0 phr

Proton site assignments (chemical shift δ: ppm relative to TMS)	T_1^H (s)								
	Unvulcanized blends				Vulcanized blends			Pure components	
	PVC/SBR 50/50	PVC/NBR-40 50/50	PVC/NBR-29 50/50	PVC/NBR-29/ SBR 50/10/40	PVC/SBR 50/50	PVC/NBR-29 50/50	PVC/NBR-29/ SBR 50/10/40		
PVC									
CHCl (57 ± 1)	2.61 ± 0.08	1.57 ± 0.02	1.57 ± 0.02	2.33 ± 0.09	2.74 ± 0.15	1.78 ± 0.07	2.36 ± 0.15	2.75 ± 0.01	
CH_2 (46 ± 1)	2.74 ± 0.14	1.53 ± 0.01	1.65 ± 0.01	2.39 ± 0.09	2.80 ± 0.14	1.75 ± 0.04	2.32 ± 0.18	2.59 ± 0.01	
Rubber								SBR	0.54 ± 0.01
CH (130 ± 1)	0.45 ± 0.03	1.56 ± 0.02	1.33 ± 0.04	0.75 ± 0.05	0.71 ± 0.01	1.16 ± 0.01	0.80 ± 0.01	NBR-29	0.89 ± 0.06
								NBR-40	0.91 ± 0.01
CH_2 (33 ± 1)	1.44 ± 0.03	1.60 ± 0.01	1.40 ± 0.01	1.46 ± 0.03	1.37 ± 0.02	1.54 ± 0.01	1.27 ± 0.01	SBR	0.64 ± 0.02
								NBR-29	0.75 ± 0.02
								NBR-40	0.94 ± 0.01

Table 2 Effect of curing agent concentration on the T_1^H (s) of PVC/NBR-29/SBR (50/10/40) blends

Proton site assignments (chemical shift δ: ppm relative to TMS)	T_1^H (s)			
	S 0.0, MBT 0.0, ZnO 0.0 phr	S 0.5, MBT 0.5, ZnO 1.0 phr	S 1.0, MBT 1.0, ZnO, 2.0 phr	S 2.0, MBT 0.5, ZnO 4.0 phr
PVC				
CHCl (57 ± 1)	2.33 ± 0.09	2.36 ± 0.15	2.27 ± 0.07	2.29 ± 0.12
CH_2 (46 ± 1)	2.39 ± 0.09	2.32 ± 0.18	2.24 ± 0.05	2.09 ± 0.12
Rubber				
CH (130 ± 1)	0.75 ± 0.05	0.80 ± 0.01	0.80 ± 0.02	0.93 ± 0.07
CH_2 (33 ± 1)	1.46 ± 0.03	1.27 ± 0.01	1.37 ± 0.02	1.37 ± 0.02

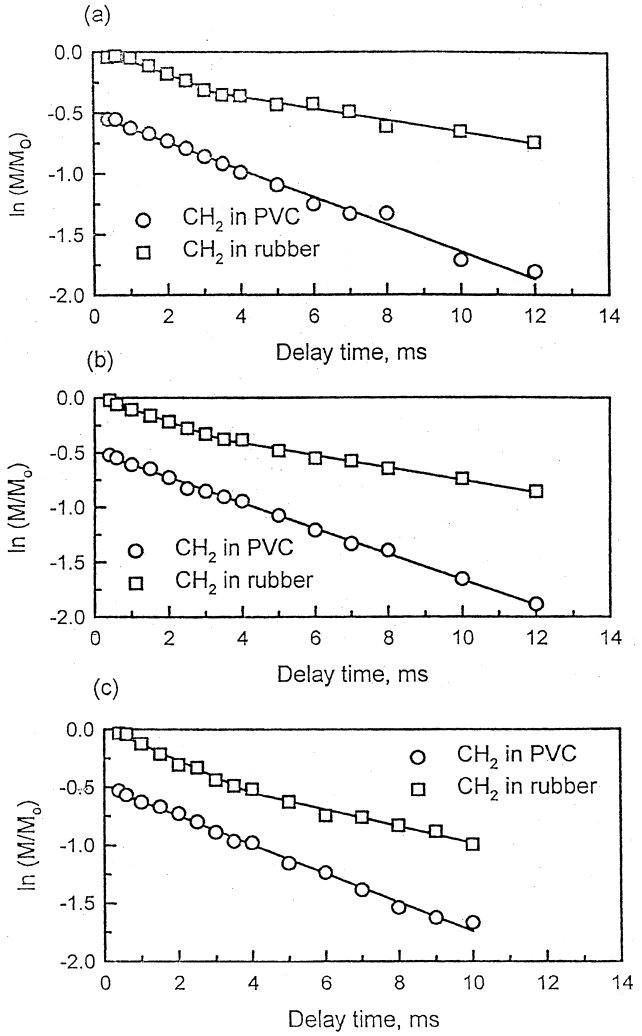

Figure 4 Semilog plots of the protonated carbon magnetization after CP as a function of delay time in $T_{1\rho}^H$ measurements for the PVC/NBR-29/SBR (50/10/40) blends: (a) unvulcanized; (b) vulcanized by S/MBT/ZnO (0.5/0.5/1.0 phr); and (c) vulcanized by S/MBT/ZnO (2.0/0.5/4.0 phr) (for clarity, the lower three lines have been shifted downward by 1.0, 1.5 and 2.0, respectively)

Figure 3 shows a magnetization decay for the unvulcanized PVC/NBR-29/SBR (50/10/40) blend, which is a ternary blend. A large difference in the relaxation times of the PVC and the rubbers can be observed from the different slopes. In the ternary blend, the increase in the T_1^H of the CH group in the rubbers, relative to that in the PVC/SBR (50/50) blend, is accompanied by a decrease in the T_1^H of the CHCl and CH_2 groups in the PVC (*Table 1*). This is due to the averaging effect of proton spin diffusion across the interface of the blends.

Table 2 lists the T_1^H for protonated carbons of ternary PVC/NBR-29/SBR (50/10/40) blends with four different sulfur concentrations. The T_1^H of PVC, especially that of the CH_2 group, decreases with increasing concentration of sulfur. It is possible that covulcanization between NBR and SBR reduces the SBR domain size, which in turn increases the degree of interpenetration and coupling between PVC and SBR at the interfacial regions. However, this is inconclusive based on T_1^H measurements alone. The proton spins of the CH and CH_2 in the rubbers relax exponentially, but their T_1^H values are not equal (c.f. *Figure 3*). The rubber T_1^H values do not show a significantly clear trend with the increase in sulfur concentration.

$T_{1\rho}^H$ *measurements*

Comparing with the $T_{1\rho}^H$ of pure PVC, the $T_{1\rho}^H$ values of the PVC in the blends are slightly longer. Before blending, the glassy PVC has a glass transition temperature above the ambient temperature and a slower relaxation rate than SBR and NBR, which have glass transition temperatures below the ambient temperature. The methine groups have only one proton attached to the carbon, and their $^1H-^{13}C$ cross polarization efficiency is lower than the methylene group. The cross polarization condition is optimized with respect to the methylene groups in the rubbers.

Figure 4 shows semilog plots of the $T_{1\rho}^H$ decay of the CH_2 group of the PVC and of the rubbers of one unvulcanized and two vulcanized PVC/NBR-29/SBR blends (S/MBT/ZnO = 0.5/0.5/1.0 and 2.0/0.5/4.0 phr). All the lines in *Figure 4a–c* show that the decay for the CH_2 group of PVC is linear, indicating a single relaxation time. However, the decay of the CH_2 group of rubbers is bimodal, reflecting a distribution of motional heterogeneities. The decay curve may be fitted to two-component decay as follows:

$$M(t) = M_0[\Phi_s \exp(-t/T_{1\rho s}^H) + \Phi_l \exp(-t/T_{1\rho l}^H)] \quad (1)$$

where $M(t)$ is the magnetization at decay time t and M_0 is the magnetization at zero spin-lock time or the thermal equilibrium value, Φ_s and Φ_l are rubber fractions associated with short $T_{1\rho s}^H$ and long $T_{1\rho l}^H$ relaxation times, respectively. The sum of Φ_s and Φ_l equals 1. At large $t > 5T_{1\rho s}^H$, the contribution from the first term on the right-hand side of equation (1) is negligible. Having calculated the long $T_{1\rho l}^H$ contribution, the short $T_{1\rho s}^H$ contribution is found by subtracting the long

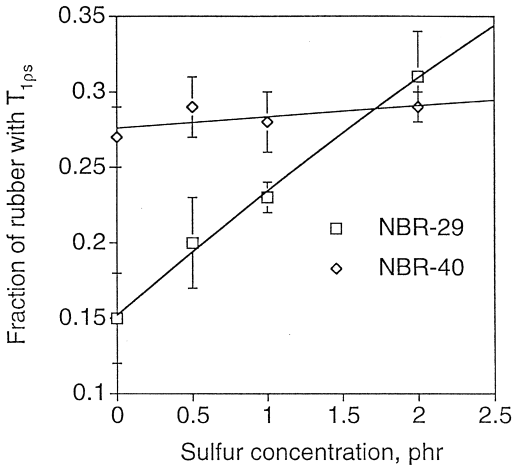

Figure 5 Rubber fractions in the vicinity of PVC as a function of curing sulfur concentration

$T_{1\rho l}^{H}$ component (i.e. the second term in equation (1)) from the observed data at shorter delay times. Physically, the rubbers can be classified into two subdomains in terms of their relaxation time in the rotating frame. The first rubber subdomain is specified by the fraction Φ_s that contributes to the shorter $T_{1\rho s}^{H}$, and the second subdomain is specified by the fraction Φ_l that contributes to the longer $T_{1\rho l}^{H}$.

The value of Φ_s is plotted as a function of the sulfur concentration in *Figure 5*. The value of Φ_s increases as the sulfur concentration increases. The Φ_s value determined by this method may not be the actual volume fraction of the rubbers with $T_{1\rho s}^{H}$ because the two rubber subdomains may have different cross polarization efficiencies and proton spin diffusion rates. Generally, cross polarization is more efficient and spin diffusion more rapid in less mobile domains. The rubber domains are large on the n.m.r. scale, as confirmed by TEM. When the spin diffusion rate is small relative to the difference between the $T_{1\rho s}^{H}$ and $T_{1\rho l}^{H}$ relaxation rates, the two rubber subdomains relax independently[23,25]. Hence, fitting equation (1) with two exponential decay functions should give an estimate on the distribution of the two rubber subdomains. However, the difference in Φ_s between the blends containing NBR-29 and NBR-40, as shown in *Figure 5*, may not necessarily mean that the NBR-40 blend has a higher concentration of rubbers in close contact with PVC than the NBR-29 blend. The differences in cross polarization efficiency and spin diffusion rate make quantitative comparisons between the Φ_s values of NBR-29 and NBR-40 blends difficult.

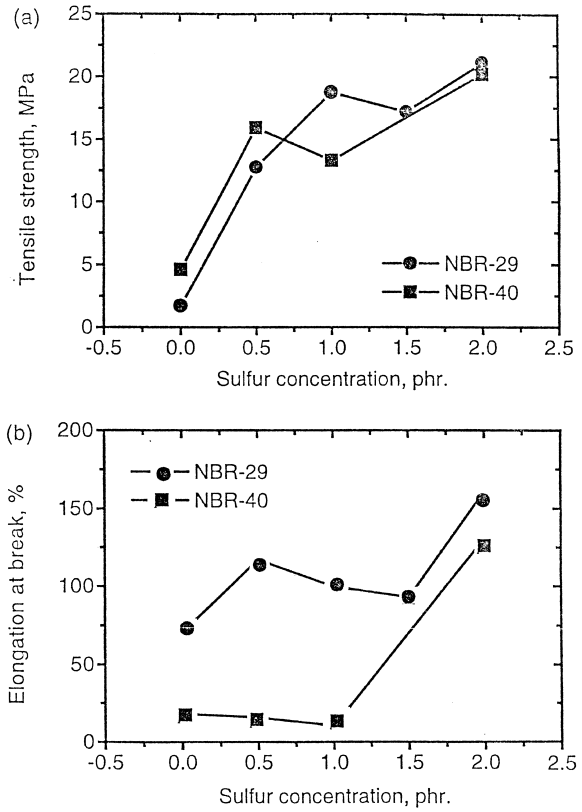

Figure 6 Tensile strength and elongation-at-break of PVC/NBR/SBR (50/10/40) blends as a function of sulfur concentration

In spite of these concerns, Φ_s seems to be a good index of the rubber concentration at the interfacial regions between the PVC and SBR phases. Tensile strength and elongation-at-break measurements of the ternary blends show similar trends as Φ_s *versus* sulfur concentration (c.f. *Figure 6*). The increase in tensile strength and elongation-at-break is attributed to the covulcanization of NBR and SBR. Covulcanization reduces the rubber domain size, and promotes a higher concentration of the rubbers and a higher degree of interpenetration between PVC and SBR at the interfacial regions.

Tables 3 and 4 summarize the $T_{1\rho}^{H}$ values of PVC and rubbers in the PVC/NBR/SBR (50/10/40) blends as a

Table 3 Effect of curing agent concentration on the proton $T_{1\rho}^{H}$ (ms) of PVC/NBR-29/SBR (50/10/40) blends

Proton site assignments (chemical shift δ: ppm relative to TMS)	S 0.0, MBT 0.0, ZnO 0.0 phr	S 0.5, MBT 0.5, ZnO 1.0 phr	S 1.0, MBT 1.0, ZnO 2.0 phr	S 2.0, MBT 0.5, ZnO 4.0 phr	Pure component	
PVC						
CHCl (57 ± 1)	7.92 ± 0.08	8.12 ± 0.10	8.02 ± 0.10	7.72 ± 0.05	7.22 ± 0.07	
CH_2 (46 ± 1)	8.80 ± 0.13	8.59 ± 0.02	8.11 ± 0.05	7.88 ± 0.06	7.86 ± 0.13	
Rubber						
CH (130 ± 1)	8.80 ± 0.95	7.76 ± 0.41	5.38 ± 0.20	3.26 ± 0.04	SBR	6.31 ± 0.54
					NBR-29	2.74 ± 0.17
CH_2 (33 ± 1)						
$T_{1\rho l}^{H}$	22.1 ± 0.8	18.3 ± 0.1	18.5 ± 0.4	18.1 ± 0.3	SBR	4.96 ± 0.18
$T_{1\rho s}^{H}$	2.18 ± 0.11	1.67 ± 0.13	1.48 ± 0.12	1.89 ± 0.16	NBR-29	2.11 ± 0.08

Table 4 Effect of curing agent concentration on the $T_{1\rho}^{H}$ (ms) of PVC/NBR-40/SBR (50/10/40) blends

Proton site assignments (chemical shift δ: ppm relative to TMS)	S 0.0, MBT 0.0, ZnO 0.0 phr	S 0.5, MBT 0.5, ZnO 1.0 phr	S 1.0, MBT 1.0, ZnO 2.0 phr	S 2.0, MBT 0.5, ZnO 4.0 phr	Pure component	
PVC						
CHCl (57 ± 1)	8.52 ± 0.01	8.49 ± 0.07	7.84 ± 0.12	7.47 ± 0.01	7.22 ± 0.07	
CH_2 (46 ± 1)	8.75 ± 0.05	8.86 ± 0.22	8.48 ± 0.15	7.95 ± 0.05	7.86 ± 0.13	
Rubber						
CH (130 ± 1)	7.05 ± 0.89	5.32 ± 0.17	4.78 ± 0.17	3.81 ± 0.20	SBR	6.31 ± 0.54
					NBR-40	1.24 ± 0.15
CH_2 (33 ± 1)						
$T_{1\rho l}^{H}$	28.9 ± 1.5	23.4 ± 0.8	24.2 ± 0.9	17.4 ± 0.1	SBR	4.96 ± 0.18
$T_{1\rho s}^{H}$	1.16 ± 0.17	2.23 ± 0.23	2.29 ± 0.10	1.80 ± 0.09	NBR-40	1.01 ± 0.02

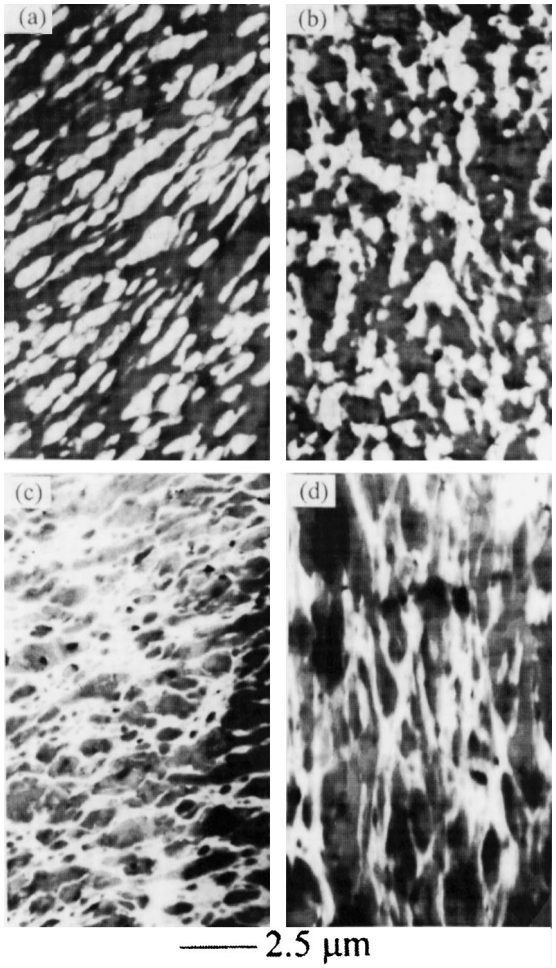

Figure 7 TEM micrographs of the OsO_4-stained sections of the PVC/NBR-29/SBR blends: (a) unvulcanized; (b) vulcanized by S/MBT/ZnO = 0.5/0.5/1.0 phr; (c) vulcanized by S/MBT/ZnO = 1.0/1.0/2.0 phr; and (d) vulcanized by S/MBT/ZnO = 2.0/0.5/4.0 phr

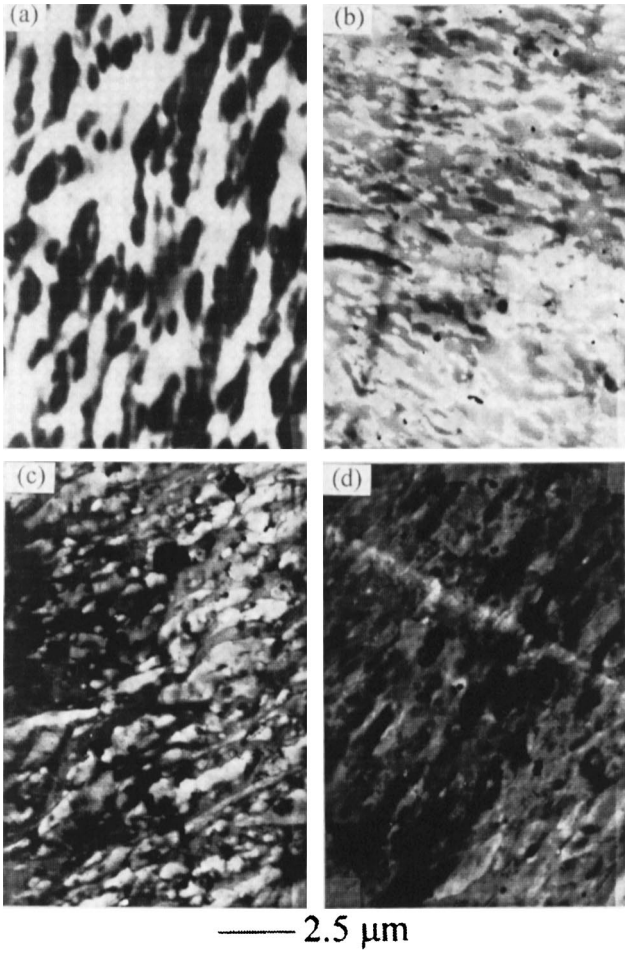

Figure 8 TEM micrographs of the unstained sections of the PVC/NBR-29/SBR blends: (a) unvulcanized; (b) vulcanized by S/MBT/ZnO = 0.5/0.5/1.0 phr; (c) vulcanized by S/MBT/ZnO = 1.0/1.0/2.0 phr; and (d) vulcanized by S/MBT/ZnO = 2.0/0.5/4.0 phr

function of the sulfur concentration. As the sulfur content increases, the CH $T_{1\rho}^{H}$ and the CH_2 $T_{1\rho l}^{H}$ values of the rubbers both decrease. The increasing constraints brought about by crosslinking may be responsible for the decrease in the $T_{1\rho}^{H}$ values. Since only a single $T_{1\rho}^{H}$ is found for the CHCl and CH_2 protons in the PVC, an enrichment of the rubbers with $T_{1\rho s}^{H}$ at the interface is necessary to enwrap and isolate the PVC from the SBR with $T_{1\rho l}^{H}$. The existence of such a PVC/rubber interface is further discussed below in our TEM study.

TEM study

Morphology of the blend. The morphology of the blends was studied by TEM. *Figure 7a–d* show the TEM micrographs for the PVC/NBR-29/SBR (50/10/40) blends with different sulfur concentrations. These samples were stained with an OsO_4 vapour. Since both SBR and NBR have double bonds, which can react with OsO_4, the dark areas are either SBR or NBR. *Figure 7a* shows the morphology of the unvulcanized blend, indicating that SBR is the

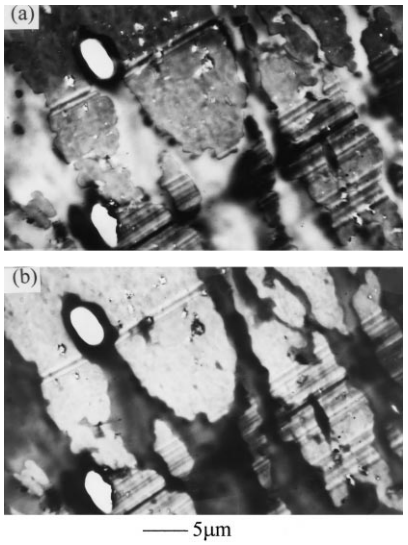

Figure 9 TEM micrographs of an unstained section of an unvulcanized PVC/SBR (50/50) blend taken after (a) 0.5 and (b) 1.0 min of exposure to the electron beam irradiation

continuous phase while PVC is the discrete phase. As the sulfur concentration increases, the particle sizes did not change much, but a phase inversion occurred — SBR changed from being the continuous phase to being the discrete phase. The phase inversion was caused by an increase in the viscosity of SBR as a result of crosslinking. *Figure 8a–d* shows the TEM micrographs for the same samples, which were not stained. In these micrographs the dark areas are the PVC phase because PVC contains Cl, which is the heaviest element in the blend. *Figures 7* and *8* provide complementary information. The detailed description of the development of the morphology with different sulfur concentrations and processing conditions will be presented in a forthcoming paper.

Interface of the blends. It is well known that polymers are sensitive to electron beam irradiation. Depending upon the molecular structure, a polymer will undergo either crosslinking or chain scission, depending on the C–H or C–C bond energy of the molecules. Double bonds of rubber under electron beam irradiation will form free radicals and crosslinks[34–37]. Upon electron beam irradiation, PVC will decompose by dehydrochlorination, resulting in a significant mass loss (up to 58 wt% based on the repeating unit of the molecule). In TEM, the mass thickness will contribute to the overall contrast observed. For unstained sections of the blends, the dark areas represent PVC because the atomic mass of Cl is high enough to cause the contrast. The contrast of the samples will slowly diminish if the concentration of the Cl in the blends decreases.

An attempt to study the interface of the blends by exposing the unstained samples under electron beam irradiation in a transmission electron microscope has been made. As discussed above, the contrast caused by the presence of Cl in PVC will slowly diminish as the concentration of Cl decreases as a result of dehydrochlorination. However, both NBR and SBR react more strongly with the electron beam than PVC. Hence, the presence of NBR, SBR or both rubbers in the PVC phase will help to slow down the dehydrochlorination process. By observing the change in the contrast of the sample under electron beam irradiation, it is possible to obtain some information about the distribution of the rubbers in the blends.

Figures 9a–b are the TEM micrographs of an unstained section of the unvulcanized PVC/SBR (50/50) blend as a function of irradiation time, in which *a* and *b* are taken at different electron bombardment times. *Figures 9a–b* are the micrographs obtained after 0.5 and 1.5 min of irradiation, respectively. Before dehydrochlorination, the PVC phase is represented by the dark areas, as shown in *Figure 9a*. The loss of HCl slowly reverses the contrast. After 1.5 min of irradiation the PVC and SBR phases are the light and dark areas, respectively. For the PVC/SBR (50/50) blend vulcanized by S/MBT/ZnO = 0.5/0.5/1.0 phr, the TEM micrographs taken after different irradiation times are shown in *Figure 10a–c*. Similar observations are made with the vulcanized blend.

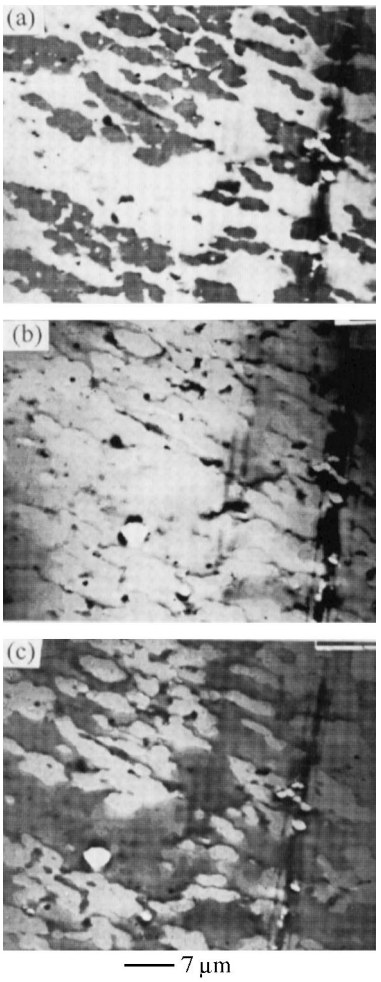

Figure 10 TEM micrographs of an unstained section of the PVC/SBR (50/50) blend vulcanized by S/MBT/ZnO = 0.5/0.5/1.0 phr taken after (a) 0.5, (b) 1.0 and (c) 2.5 min of exposure to electron irradiation

Figure 11a–c shows the TEM micrographs of an unstained section of the unvulcanized PVC/NBR-29/SBR (50/10/40) blends at several irradiation times. As the PVC decomposes under the electron beam, the contrast between the components decreases; however, in this case dark rings are observed between the PVC and SBR phases and they are still visible even after 2.5 min of irradiation. The enrichment of rubbers at the interface effectively reduces the decomposition rate of PVC[34]. The dark rings are not observed for either the unvulcanized or vulcanized PVC/SBR (without NBR as the compatibilizer) samples. The presence of the dark rings in this unvulcanized PVC/NBR-29/SBR blend confirms that the rubber enrichment at the interface is a result of the compatibilization effect of NBR. *Figure 12a–c*

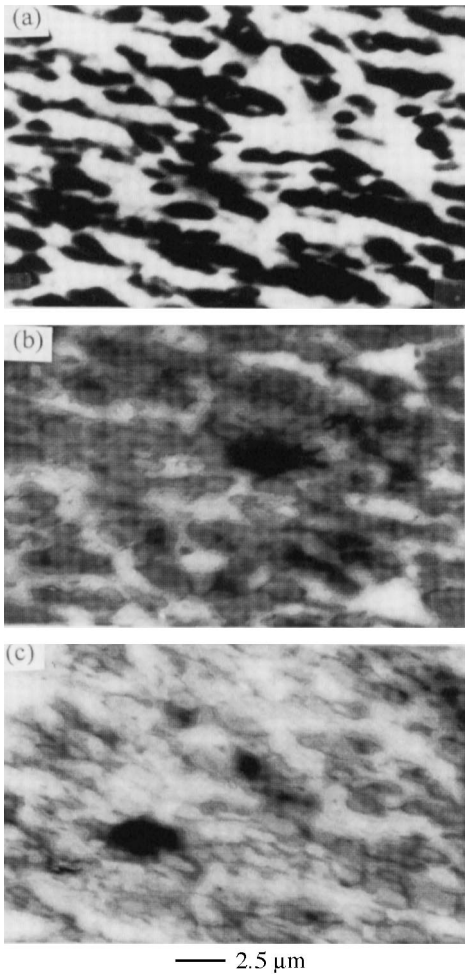

Figure 11 TEM micrographs of an unstained section of an unvulcanized PVC/NBR-29/SBR (50/10/40) blend taken after (a) 0.5, (b) 1.0 and (c) 2.5 min of exposure to the electron beam irradiation

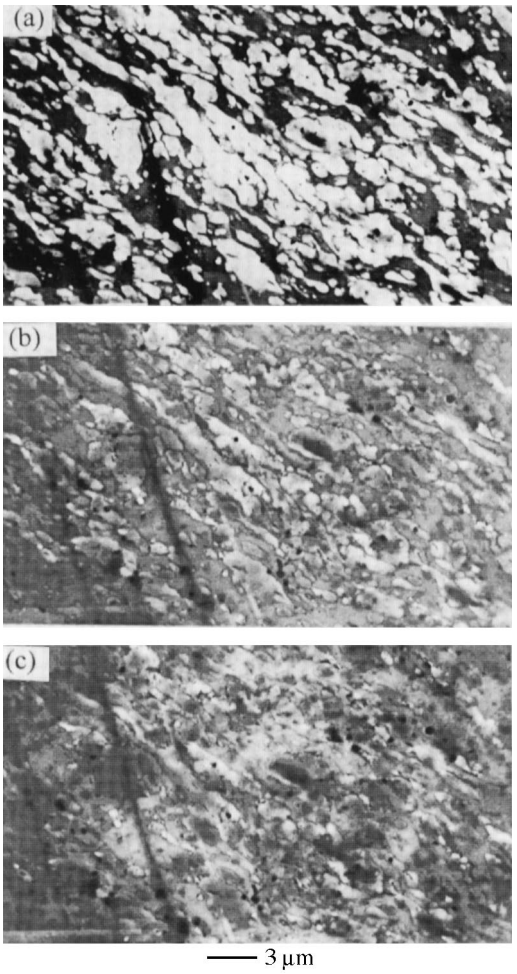

Figure 12 TEM micrographs of an unstained section of a PVC/NBR-29/SBR (50/10/40) blend vulcanized by S/MBT/ZnO (1.0/1.0/2.0) taken after (a) 0.5, (b) 1.0 and (c) 2.5 min of exposure to the electron beam irradiation

are the TEM micrographs of an unstained section of the vulcanized (S/MBT/ZnO = 1.0/1.0/2.0 phr) PVC/NBR-29/SBR (50/10/40) blend. *Figure 12a* shows that SBR is the discrete phase with a much finer particle size as compared with that of PVC shown in *Figure 11a*. In this sample, SBR is the dispersed phase because of the increase in the viscosity of SBR as a result of vulcanization. The dark rings between the SBR and PVC phases are observed even after 2.5 min of irradiation. Although it is difficult to quantify the amount of rubbers at the interface regions, the results shown in *Figures 11* and *12* confirm that the rubber concentrations at the interfacial regions are higher, thus stabilizing the decomposition of PVC. The TEM micrographs of the unstained samples for this blend system provide a unique method to show the segregation of the rubbers at the interfacial regions between PVC and SBR for the compatibilized blends.

CONCLUSIONS

(1) The spin-lattice relaxation times both in laboratory and rotating frames were used to analyze the morphology of the blends. Exponential T_1^H decay was found for all the protons in unvulcanized PVC/NBR-40 blends, while the T_1^H values for the rubber and the PVC are slightly different for the PVC/NBR-29 blends.
(2) Two $T_{1\rho}^H$ components were found for the rubber methylene of the ternary PVC/NBR/SBR (50/10/40) blends. The short $T_{1\rho}^H$ component is associated with the rubbers in the proximity of the PVC. As the sulfur concentration increases, the fraction of rubbers with short $T_{1\rho}^H$ increases.
(3) TEM micrographs for the samples stained by OsO_4 show that a phase inversion occurs for the PVC/NBR-29/SBR blends as the sulfur concentration increases.
(4) TEM micrographs for the unstained samples show identical morphological patterns to the stained ones. Their contrasts are unstable and fade away under electron beam bombardment. The uncompatibilized blends show contrast inversion after only 2 min of electron beam bombardment due to rapid dehydrochlorination. However, in the compatibilized blends, the rubber in close proximity of the PVC can stabilize the PVC and reduce the rate of dehydrochlorination. The enhanced rubber concentration at the interface between the PVC and SBR phases of the compatibilized blends is demonstrated by the observation of dark rings at the interface.
(5) Both n.m.r. and TEM results show an enhanced concentration of rubber(s) at the interface between PVC and SBR.

ACKNOWLEDGEMENTS

This work was supported by the Hong Kong Government

Research Grant Council under the grant number HKUST 582/95P. We thank Kit Chan of the Materials Characterization and Preparation Facility at the Hong Kong University of Science and Technology for her help in the n.m.r. experiments.

REFERENCES

1. Maciel, G. E. (ed.), *Nuclear Magnetic Resonance in Modern Technology*. Kluwer Academic Publishers, Dordtrecht, 1992.
2. Ibbett, R. N., *n.m.r. Spectroscopy of Polymers*. Blackie Academic and Professional, Glasgow, 1993.
3. McBrierty, V. J. and Packer, K. J., *Nuclear Magnetic Resonance in Solid Polymers*. Cambridge University Press, Cambridge, 1993.
4. Schaefer, J. and Stejskal, E. O., *J. Am. Chem. Soc.*, 1976, **98**, 1031.
5. Schaefer, J., Sefcik, M. D., Stejskal, E. O. and Mckay, R. A., *Macromolecules*, 1981, **14**, 188.
6. Stejskal, E. O., Schaefer, J., Sefcik, M. D. and Mckay, R. A., *Macromolecules*, 1981, **14**, 275.
7. Caravatti, P., Deli, J. A., Bodenhausen, G. and Ernst, R. R., *J. Am. Chem. Soc.*, 1982, **104**, 5506.
8. Caravatti, P., Neuenschwander, P. and Ernst, R. R., *Macromolecules*, 1985, **18**, 119.
9. Caravatti, P., Neuenschwander, P. and Ernst, R. R., *Macromolecules*, 1986, **19**, 1889.
10. Schmidt-Rohr, K. and Spiess, H. W., *Multidimensional Solid-State n.m.r. and Polymers*. Academic Press, London, 1994.
11. Kwak, S.-Y., Kim, S. Y. and Nakajima, N., *J. Polym. Sci.*, 1997, **B35**, 709.
12. Afeworki, M., Mckay, R. A. and Schaefer, J., *Mater. Sci. Eng.*, 1993, **A162**, 221.
13. Tomaselli, M., Meier, B. H., Robyr, P., Suter, U. W. and Ernst, R. R., *Chem. Phys. Lett.*, 1993, **205**, 145.
14. Tezuka, A., Takegoshi, K. and Hikichi, K., *J. Molecular Structure*, 1995, **355**, 1.
15. Mansfeld, M. and Veeman, W. S., *Chem. Phys. Lett.*, 1994, **222**, 422.
16. Munie, G. C., Jonas, J. and Rowland, T. J., *J. Polym. Sci. Polym. Chem. Ed.*, 1980, **18**, 1061.
17. Harrison, D. J. P., Yates, W. R. and Johnson, J. F., *JMS-Rev. Macromol. Chem. Phys.*, 1985, **C25**, 481.
18. Lyerla, J. R., in *High Resolution n.m.r. Spectroscopy of Synthetic Polymers in Bulk*, ed. R. A. Komoroski. VCH Publishers, Florida, 1986.
19. Komoroski, R. A., in *High Resolution n.m.r. Spectroscopy of Synthetic Polymers in Bulk*, ed. R. A. Komoroski. VCH Publishers, Florida, 1986.
20. Axelson, D. E., in *High Resolution n.m.r. Spectroscopy of Synthetic Polymers in Bulk*, ed. R. A. Komoroski. VCH Publishers, Florida, 1986.
21. Laupretre, F., Bokobza, L. and Monnerie, L., *Polymer*, 1993, **34**, 468.
22. Le Menestrel, C., Kenwright, A. M., Sergot, P., Laupretre, F. and Monnerie, L., *Macromolecules*, 1992, **25**, 3020.
23. Douglass, D. C. and McBrierty, V. J., *Macromolecules*, 1978, **11**, 766.
24. McBrierty, V. J., Douglass, D. C. and Kwei, T. K., *Macromolecules*, 1978, **11**, 1265.
25. Veeman, W. S. and Maas, W. E. J. R., in *Solid-State n.m.r. III: Organic Matter*, ed. B. Blumich. Springer-Verlag, Berlin, 1994.
26. Fukumori, K., Sato, N. and Kurauchi, T., *Rubber Chem. and Techn.*, 1991, **64**, 522.
27. Kwak, S.-Y. and Nakajima, N., *Polymer*, 1996, **37**, 195.
28. Henrichs, P. M., Tribone, J., Massa, D. J. and Hewitt, J. M., *Macromolecules*, 1988, **21**, 1282.
29. Lindberg, K. A. H., Vesely, D. and Bertilsson, H. E., *J. Mater. Sci.*, 1989, **24**, 2825.
30. Lindberg, K. A. H., Vesely, D. and Bertilsson, H. E., *J. Mater. Sci.*, 1985, **20**, 2225.
31. Van Gisbergen, J. and Overbergh, N., in *Radiation Processing of Polymers*, ed. A. Singh and J. Silverman. Hanser, New York, 1992, p. 51.
32. Nguen, T. Q. and Kausch, H. H., *J. Appl. Polym. Sci.*, 1984, **29**, 455.
33. Van Gisbergen, J. G. M., Borgmans, C. P. J. H., Van der Sanden, M. C. M. and Lemstra, P. J., *Polym. Commun.*, 1990, **31**, 162.
34. Zhu, S.-H. and Chan, C.-M., *Macromolecules*, 1998, **31**, 1690.
35. Van Gisbergen, J. G. M., Meijer, H. E. H. and Lemstra, P. J., *Polymer*, 1989, **30**, 2153.
36. Van Gisbergen, J. G. M. and Meijer, H. E. H., *J. Rheol.*, 1991, **35**, 63.
37. White, J. R., Chapman, J. N. and McVitier, S., *J. Polym. Sci.*, 1991, **29**, 31.
38. Mascia, L. and Moggi, A., *J. Polym. Sci. Part B*, 1993, **31**, 1309.
39. Gao, X. Y. and Rempel, G. L., *Macromolecules*, 1992, **25**, 883.
40. Tonelli, A. E., *n.m.r. Spectroscopy and Polymer Microstructure: The Conformational Connection*. VCH Publishers, New York, 1989.